京都大学防災研究所年報　第44号 B-2　平成13年4月
Annuals of Disas. Prev. Res. Inst., Kyoto Univ., No.44 B-2, 2001

A rainfall-sediment-runoff model in the upper Brantas River, East Java, Indonesia

TAKARA Kaoru, NAKAYAMA Daichi, TACHIKAWA Yasuto,
SAYAMA Takahiro*, NAKAGAWA Hajime, SATOFUKA Yoshifumi,
EGASHIRA Shinji** and FUJITA Masaharu***

*Graduate School of Engineering, Kyoto University
**Fuculty of Science and Engineering, Ritsumeikan University
***Graduate School of Agriculture, Kyoto University

Synopsis

A distributed rainfall-sediment-runoff model is constructed to investigate flood and sediment movement on a catchment scale. The model treats spatial data sets such as topography and land cover effectively by applying GIS (geoglaphical information system) and remote sensing techniques. This research uses GIS to produce a DEM (digital elevation model) and remotely sensed data to classify land cover. The model constructed here is a grid-cell-based distributed model. The grid-cell-based kinematic wave model calculates rainfall-runoff and sediment is yielded when overland flow occurs on each grid-cell with surface volcanic soil layer. A primitive model (Takara, 2000) assumed that sediment was yielded with infiltration depth D regardless of energy of overland flow, which has limitation to transport sediment on each grid-cell. Considering a transportation capacity of overland flow on each grid-cell makes it possible to model both sediment yield processes and sediment deposit processes. The unit stream power theory decides the transportation capacity. Yielded sediment in slope grid-cells moves in the flow direction derived from the DEM to river grid-cells, on which bed load and suspended load are calculated. The model is applied to the Lesti River basin (625 km^2) located in the upper Brantas River basin, and simulates sediment runoff during a rainy season from November 1995 to April 1996.

Keywords *: Brantas River; rainfall-sediment-runoff model; unit stream power; GIS; ADEOS/AVNIR*

1. Introduction

The Brantas River (Fig.1) is the second largest river in Java Island, Indonesia. The length is 320 km and the catchment area is 12,000 km^2. It originates from the southwestern slope of Mt. Arjuno and flows out into the Madura Strait. The basin consists of active volcanic mountains; for example Mt. Kelud erupts once every 15-30 years and Mt. Semeru emits a lot of smoke continuously. Hundreds million cubic meters of volcanic materials flow down the surrounding slopes when

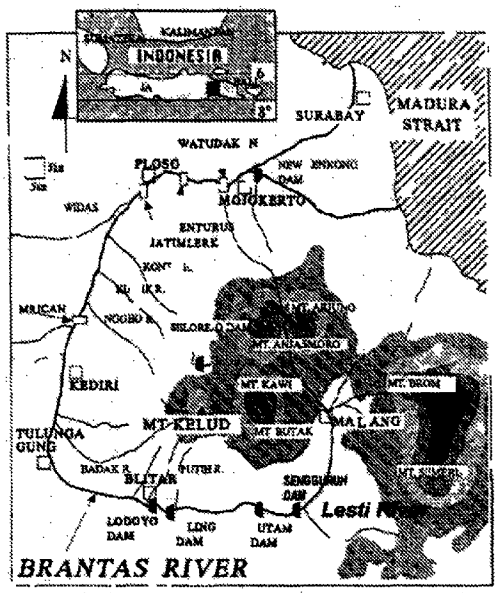

Fig. 1 Brantas River basin (Egashira et al., 1997)

these volcanoes erupt. The basin is covered with volcanic ash or the geologic stratum consists of volcanic debris. Heavy rainfall and runoff in the rainy season from November to April are the major cause of a large amount of sediment yield, which is deposited in reservoirs and riverbeds.

Sediment from the Lesti River basin studied here accounts for a large amount of sedimentation in the upper Brantas River. It originates Mt. Semeru (3,676 m) and drains the area of 625 km^2. The Sengguruh dam, which locates at the junction of the Lesti River and the Brantas River, was constructed in 1988 for water resources and power generation with gross storage of 21.50 million m^3, but the storage has been decreased to only 3.37 million m^3 for 8 years after the dam construction. The sedimentation at the Senggruh dam decreases the life time of the dam and increases the risk of flood.

This paper describes a distributed rainfall-sediment-runoff model, which is capable of considering spatial hydrological and geological information. This type of model is useful for prediction of sedimentation in reservoirs and riverbeds and would contribute to severe sedimentation problems caused by land use change and deforestation.

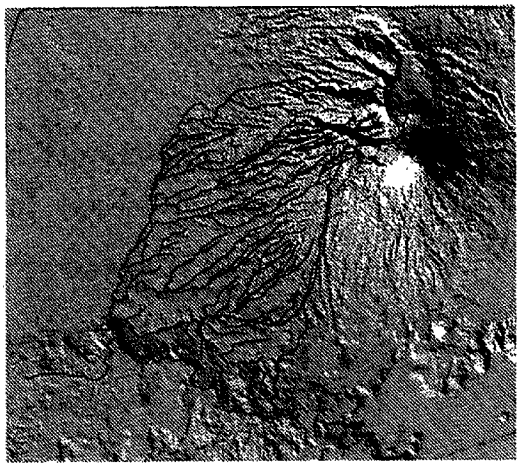

Fig. 2 50-m DEM image with river channel network and watershed boundary

2. Application of GIS and RS to hydrological modeling

Geographical Information System (GIS) is capable to take advantage of digitized geographical information using computer effectively. Applied to various fields such as urban planning, environmental planning, resource management and facility management, it is also expected as a useful tool to deal with distributed geographical data for hydrological analysis. Geophysical spatial data sets such as flow direction, slope and land cover on each grid-cell are necessary to develop the distributed hydrological models. This research uses GIS for generating DEM by plotting of contour lines and treating spatial data sets.

Remote sensing (RS) is one of the powerful tools for observing and monitoring geomorphologic and hydrologic conditions on the land surface. This paper classifies land cover of the Lesti River basin using ADEOS/AVNIR image (spatial resolution 16 m) acquired on June 4, 1997 with the maximum likelihood classification method.

2.1 DEM and flow direction paths derived with GIS

From digitized contour lines on a 1:50,000 topographical map, ERDAS/IMAGINE generates Triangulated Irregular Network (TIN) and transforms it to a square-grid DEM with any resolution. Figure 2 shows the shaded DEM image of 50-m resolution.

Flow direction on each grid-cell is decided

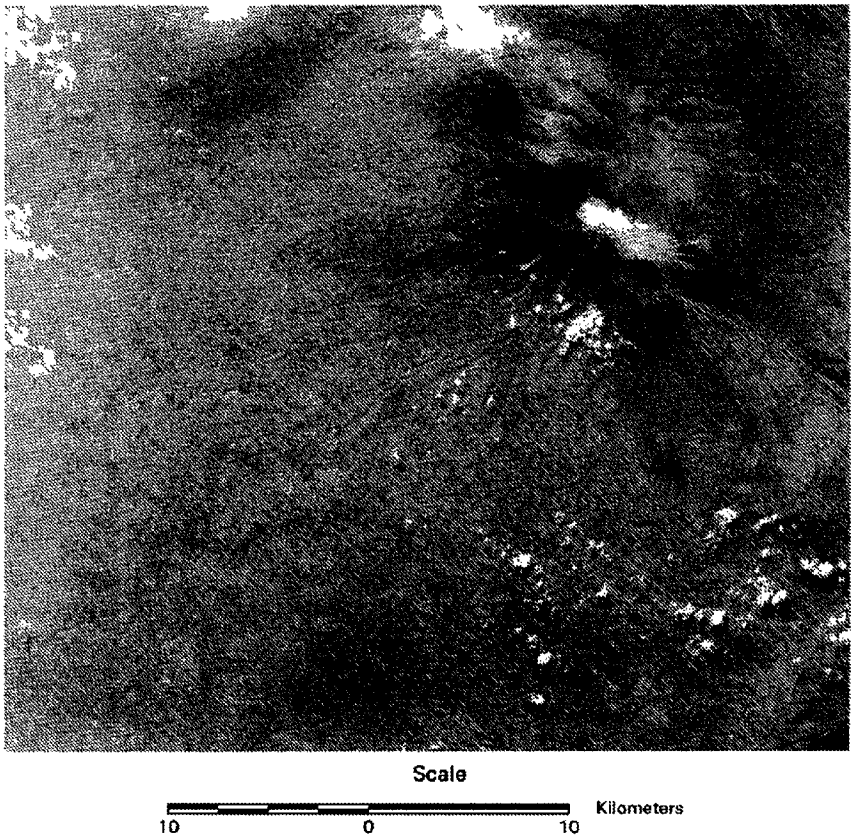

Fig. 3 ADEOS/AVNIR image (June 4, 1997)

based on the DEM. Since the location and the density of the river channel and the boundary of watershed are important for runoff analysis, the digitized river channel and the watershed boundary maps were piled on other maps on GIS as shown in Fig. 2 . The procedure to make the flow direction map is as follows.

1. The GIS transforms the vector layers of the river channel and the watershed boundary into the raster layer which has the same resolution as the DEM.
2. To define the connection of the river grid-cells, the flow direction in the river is decided at first.
3. The flow directions on slope-cells are calculated. The elevation of the watershed boundary cells are raised to prevent flow paths from crossing the watershed boundary.

2.2 Land cover classification using ADEOS/AVNIR

An earth observation satellite ADEOS, which was developed by the National Space Development Agency of Japan (NASDA), was launched on August 17, 1996 into a solar-synchronous subrecurrent orbit with a recurrent period of 41 days at an attitude of about 800 km. It had been available for 10 month by June 30, 1997. ADEOS carried six sensors for consolidated continuous measurement of land, sea and air, the Advanced Visible and Near-Infrared Radiometer (AVNIR), the Ocean Color and Temperature Scanner (OCTS) and so on.

AVNIR is a visible and near-infrared radiometer to measure land and costal zones with high spatial resolution (16 m). It monitors environmental phenomena such as vegetation and desertification.

In this research, we used an AVNIR image (Fig. 3) acquired on June 4, 1997 for cathment land cover classification. Classification by a supervised method needs training area. We referred to the land cover map published in 1989 for extracting the training areas. Figure 4 shows the land cover classification map obtained by the maximum likelihood classification technique. It shows that most of the Lesti River basin is classified into

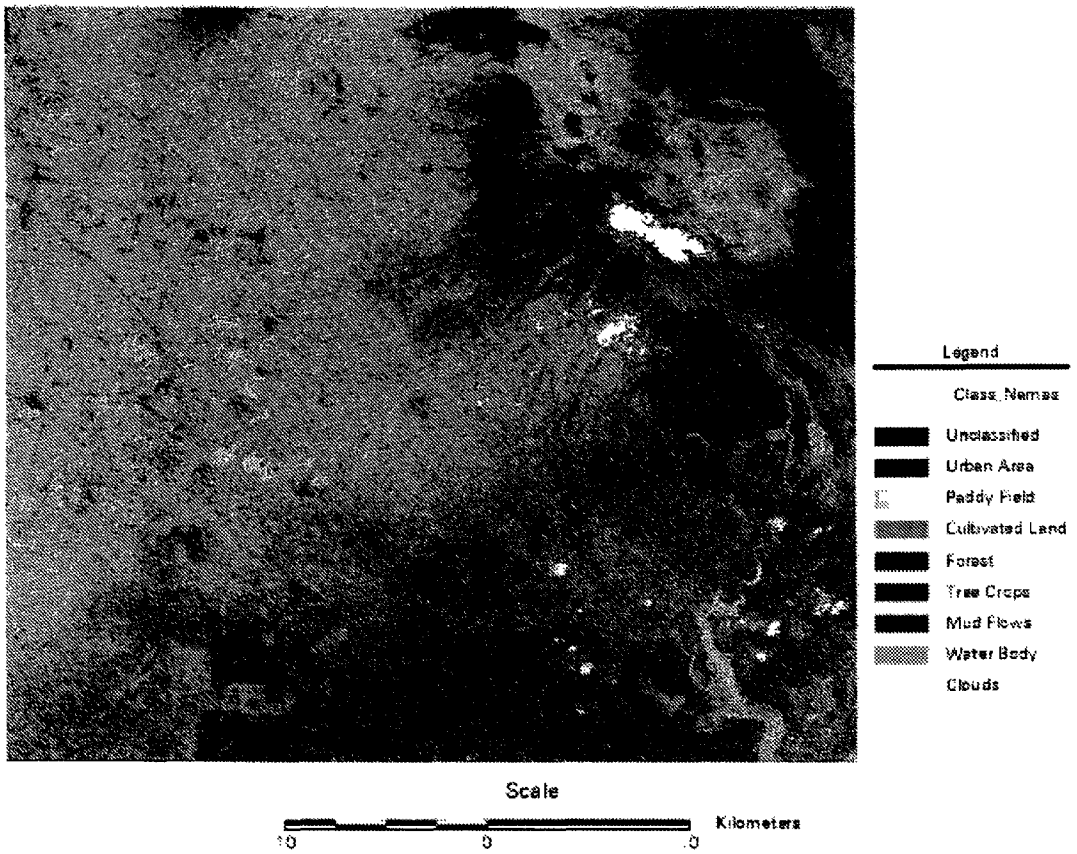

Fig. 4 Land cover classification map

'Cultivated Land' and 'Tree Crops' classes. 'Tree Crops' is located in the area where the elevation is from about 1000 m to 1500 m, and 'Cultivated Land' is on the lower area than that. Roedjito and Harianto (1995) reported that 70 to 80 % of the Lesti River basin has been cultivated to produce maize, potatoes, and cassavas under 1000 m area. This agrees with the result of land cover classification by RS, which is also confirmed by our field survey in January 2001. Note that there is some difficulty to identify the 'Paddy Field' class because the surface conditions of the paddy fields are different from field to field even at the same time. In addition, cloud covers at the top of the Mt. Semeru, which is the out of the Lesti River basin, causes some error there.

3. A distributed sediment-runoff model

3.1 The concept of the model

A spatially distributed model has to be constructed for considering the sediment movement on a catchment scale. Volcanic ash areas like the Brantas River basin may yield sediment on the cultivated lands, forests, and even urban areas. The overland flow is easy to occur in the volcanic sediment area, and the overland flow yields sediment (Jitousono and Shimokawa, 1989). The kinematic wave runoff (KWR) model simulates rainfall-runoff on each grid-cell which has the same resolution as DEM (250 m), and the sediment is assumed to be yielded when over land flow occurs. A primitive model (Takara, 2000) assumed that the sediment was yielded with infiltration depth D regardless of energy of overland flow, but overland flow has limitation to transport sediment on each grid-cell. This research considers the transportation capacity of overland flow on each grid-cell to model not only sediment yield process but also sediment deposit process physically. The transportation capacity is calculated based on the unit stream power (USP) theory. Yielded sediment in slope cells moves in the flow direction derived from the DEM to river grid-cells, on which bed load and suspended load are calculated. The model is applied to the Lesti River basin (625 km^2) located in

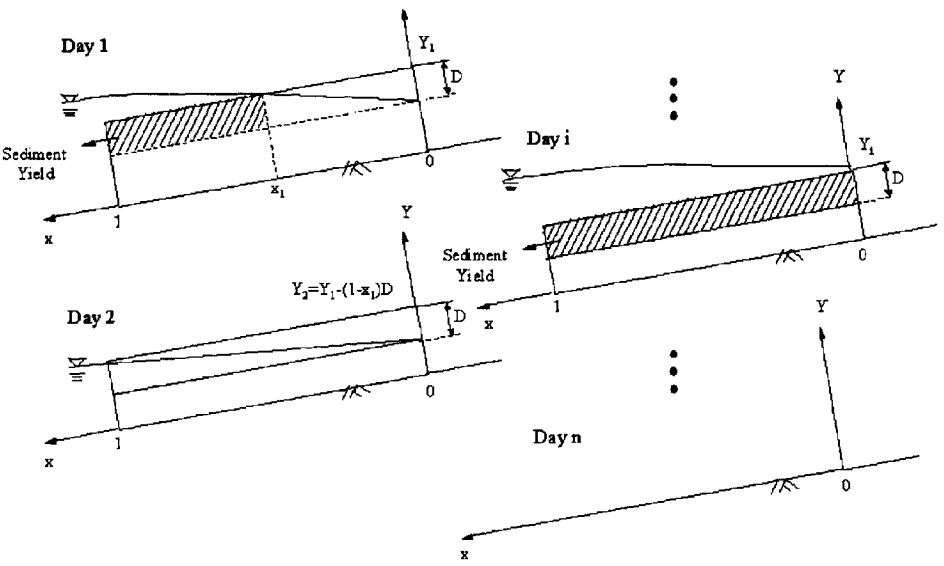

Fig. 5 Primitive sediment-runoff model (Takara, 2000)

the upper Brantas River basin, and simulates sediment runoff from November 1995 to April 1996.

3.2 Kinematic Wave model

The KWR model is expressed by the following equations.

$$\frac{\partial h}{\partial t} + \frac{\partial q}{\partial x} = r(x,t) \tag{1}$$

$$q = \begin{cases} ah & : \ h < d \\ \alpha(h-d)^m + ah & : \ h \geq d \end{cases} \tag{2}$$

The initial and boundary conditions are respectively given:

$$h(x,0) = H_1(x), \qquad 0 \leq x \leq L \tag{3}$$

$$h(0,t) = H_B(x), \qquad t > 0 \tag{4}$$

where $a = k\sin\theta/\gamma$; q : discharge per unit width; h : water depth on the slope; r : rainfall intensity; $d = \gamma D$ (γ : porosity; D : infiltration depth); t : time; x : location from the upper boundary and α, m are constant values : $m = 5/3$, $\alpha = \sin^{\frac{1}{2}}\theta/n$ (n : Manning coefficient).

3.3 Primitive sediment-runoff model

Figure 5 explains the concept of primitive sediment-runoff model. Each grid-cell is regarded as a slope covered with volcanic ash with a uniform depth of Y. The rainwater falling on the slope penetrates the volcanic ash up to the depth D from the surface. Subsurface and surface (overland) runoffs are taken into account; if the overland flow occurs then the sediment indicated by hatching in Fig. 5 flows out. When the surface runoff occurs at the top of the cell (as shown in Day i) in the middle of mountain slope, all the surface ash up to the depth D will flow out. At the beginning of Day 2, the surface layer depth is averaged over the slope then sediment is yielded if overlandflow occurs. Repeating this process, finally the surface layer will disappear as shown in Day n. in Fig. 5 .

4. Sediment-runoff model based on USP theory

The primitive model assumed the sediment to be yielded with infiltration depth D. This assumption cannot consider the sediment deposit process or the influence of the velocity of overland flow during the sediment yield process. Treating the transportation capacity (TC) of the overland flow on each grid-cell, which calculated by the unit stream power (USP) theory for sediment yield, this paper makes it possible to model the sediment deposit process and calculate the volume of the sediment physically. Figure 6 explains the concept of this model.

4.1 Unit stream power theory

The USP theory contributing to the transportation capacity of sediment is defined as a product of mean velocity V and slope S. The upper

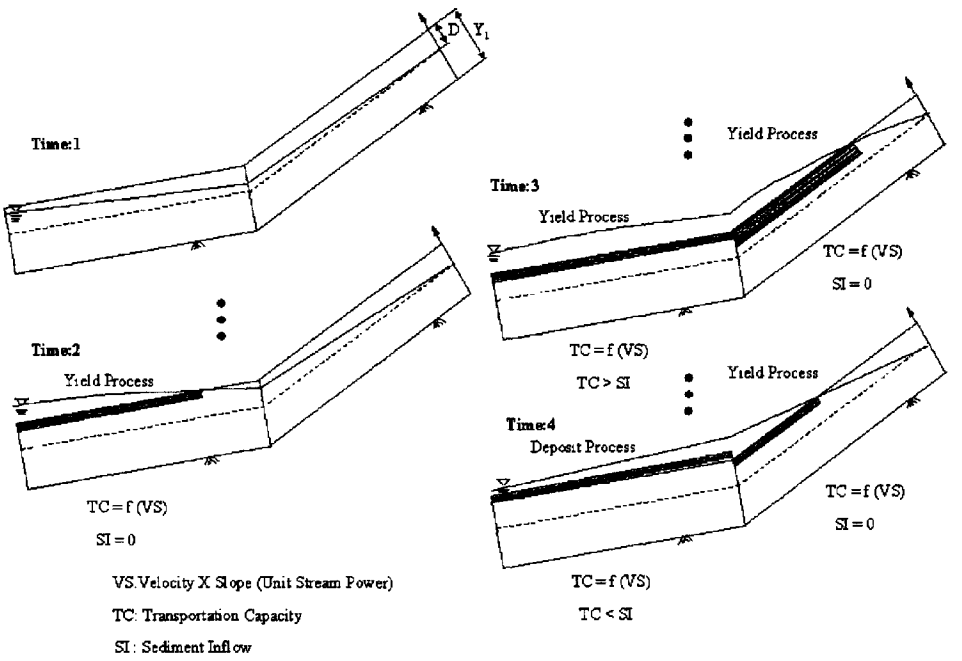

Fig. 6 USP sediment-runoff model

limit to the sediment concentration in the overland flow C_t is calculated as follows:

$$\log C_t = I + J(\frac{VS}{\omega} - \frac{V_{cr}S}{\omega}) \qquad (5)$$

where I,J : non-dimension values decided by experiment; $V_{cr}S$: critical unit stream power; ω : fall velocity of sediment (0.050 m/sec). We used the value suggested by Moore and Burch (1986) for the sheet erosion : I=5.0105, J=1.363.

4.2 Sediment yield and deposit process

The KWR model simulates the mean velocity V and the discharge Q on each grid-cell with 1-hour time step. The C_t is calculated by the Eq.(5), and the TC is the product of the C_t and Q. If the volume of sediment supplied (SI) from upper grid-cell is bigger than the TC, sediment of TC-SI will be yielded. On the other hand, the sediment from the upper grid-cell will be deposited with the volume of SI-TC when SI is bigger than TC because overland flow is not capable to move all of sediment from upper grid-cells.

5. Sediment transportation analysis in river channel

A single channel is taken into account in each grid-cell of 'River' land cover class. The channel width is assumed to be 1 m to 25 m, which depends on the distance from the catchment outlet. Rainfall over the 'River' grid-cell is directly input to the channel as lateral inflow. The sediment which reaches to the 'River' grid-cell is transported in the channel to downstream as bed load and suspended load. The transportation depends on the discharge in the channel computed by the KWR model for channels.

The bed load is computed by the equation proposed by Ashida and Michiue (1972):

$$q_{bb} = 17\sqrt{sgd^3}\tau_{*e}^{3/2}\left(1-\frac{\tau_{*c}}{\tau_*}\right)\left(1-\frac{u_{*c}}{u_*}\right) \qquad (6)$$

where

$$\tau_* = u_*^2/sgd$$
$$\tau_{*c} = u_{*c}^2/sgd$$
$$\tau_{*e} = u_{*e}^2/sgd$$
$$u_* = \sqrt{gRI}$$
$$u_{*e} = u/\left\{6.0 + 5.75\log_{10}\frac{R}{d(1+2\tau_*)}\right\}$$
$$s = \sigma/\rho - 1$$

where σ : mass density of the sediment (2.65 g/cm^3); ρ : mass density of water (1.0 g/cm^3); g : gravity acceleration (9.81 m/s^2); d : grain size (0.4 mm); τ_* : non-dimensional shear stress; τ_{*c}:

non-dimensional critical shear stress; τ_{*e} : non-dimensional effective shear stress ($\cong$ 0.05); u_* : shear velocity ; u_{*c} : critical shear velocity; u : depth averaged velocity and R : hydraulic radius.

The suspended load transport rate is expressed as the depth-integration of the product of the mean velocity and the concentration distribution (Lane, 1941):

$$q_{bs} = uC_a \frac{h}{6Z}\left(1 - e^{-6Z} e^{6Za/h}\right) \quad (7)$$

$$Z = \frac{w_0}{\beta \kappa u_*} \quad (8)$$

where $Z = \omega_o/\beta\kappa u_{*e}$; C_a : concentration at the reference level $z = a$ (a=0.05h); ω_o : setting velocity or fall velocity; κ : Karman's constant (0.4); β: constant (1.2).

Consequently, from Eqs.(6) and (7) we obtain the sediment yield from a slope cell:

$$q_b = q_{bb} + q_{bs} \quad (9)$$

For a 'River' cell, we can obtain q_in from the slope cells associated with and the upstream 'River' cells and q_out to the downstream 'River' cell q_s at every time step.

6. Application to the Lesti River basin

6.1 Sediment problem at the Lesti River basin

The Lesti River basin (625 km^2) is located at the upper Brantas River basin. The Lesti River flows together the Brantas main river at Senggruh dam constructed in 1988. The Senggruh dam contributing to reduce the sediment deposit at Karangkates Reservoir just downstream of the Senggruh dam has gross storage capacity of 21.5 million m^3, effective storage capacity of 2.5 million m^3 and designed dead storage capacity of 19 million m^3. According to a local survey in 1996, accumulated sedimentation at the Senggruh dam was already 19 million m^3 and Roedjito & Harianto (1995) report the annual sediment runoff from the Lesti River basin is 1.37 million m^3.

6.2 Simulation conditions

In this paper we apply the rainfall-sediment-runoff model to the Lesti River basin and simulate the sediment runoff during a rainy season by inputting the observed hourly rainfall data from November 1995 to April 1996. An infiltration depth D and an initial sediment depth Y are assumed as D=10 mm and Y=500 mm respectively. The runoff coefficients and roughness indices are decided based on the landcover of each grid-cell.

7. Results and Discussions

7.1 Rainfall-sediment runoff at the outlet

Inputting the hourly effective rainfall to the primitive model and the USP model for the Lesti River basin, we simulated hourly sediment-runoff as well as rainfall-runoff for a rainy season. The effective rainfall is the product of rainfall and runoff coefficients to express the influence of evapotranspiration and infiltration loss. Figure 7 shows the hyetograph, hydrograph and sediment runoff at the outlet simulated by two models. Since the difference between the primitive model and the USP model affects to the sediment, hydrographs simulated by two models are completely the same. Despite inputting the effective rainfall, some simulated peaks are bigger than observed peaks. These differences due to the assumption of spatially-uniform rainfall over the whole basin, although the actual rainfall area should be smaller than the basin. Cumulative sediment runoff at the outlet simulated by two models is shown in Fig. 7 . The temporal variation of sediment runoff that more on rainy days and less on dry days is well simulated. Accumulated sediments at the outlet simulated by two models are around 100 million m^3 after a rainy season, and these are reasonable volume compared with the measured data.

7.2 Simulation by primitive model

Figure 8 shows the temporal change of spatial distribution of sediment by the Primitive model. The sediment depth decreases as the sediment is yielded on each grid-cell from the initial sediment depth: Y=50 cm, and in the case of using the USP model, sediment depth in some grids increases as the sediment is deposited. Figure 8 indicates that sediment yields on steep slope grid-cells are smaller than that on gentle slope grid-cells because overland flow is easy to occur on the gentle slope grid-cells. This seems to be disagree with the common idea that steep slope yields more sediment once overland occurs. Another problem lying on the primitive model is that the total volume of sediment yield is too big; about 100 times as much as

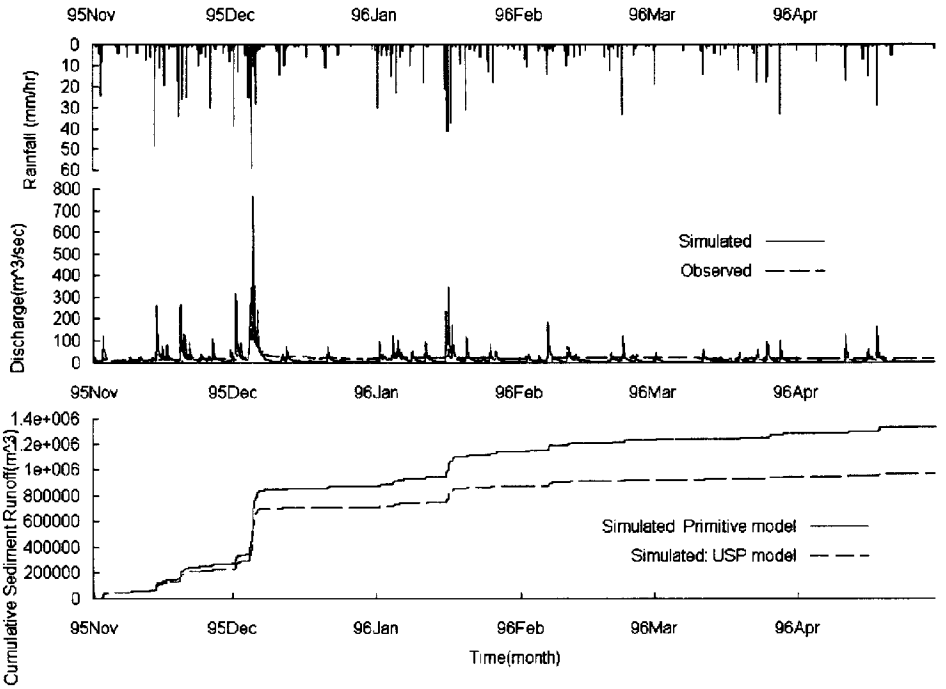

Fig. 7 Sediment runoff at the outlet of the Lesti River basin

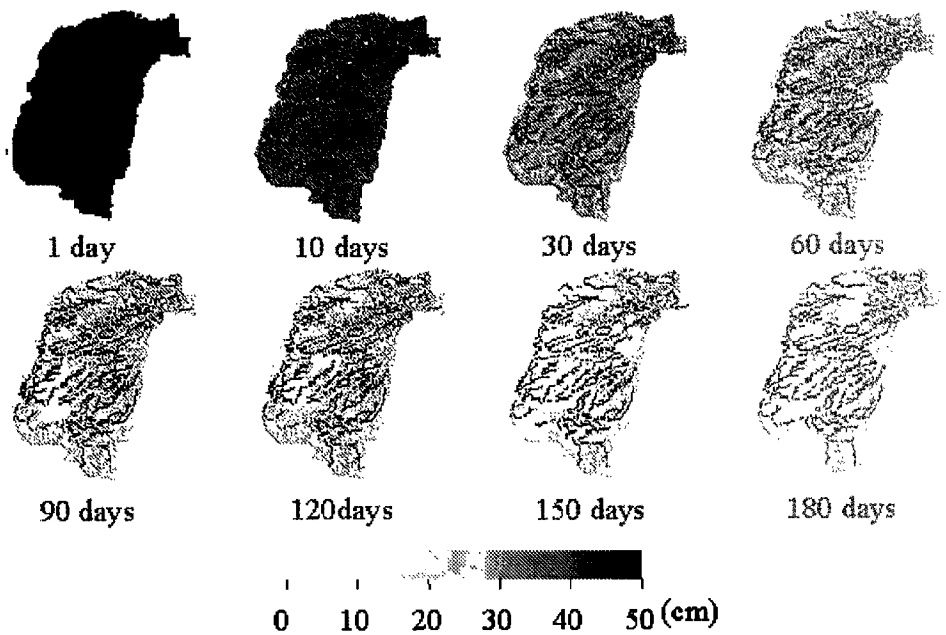

Fig. 8 Sediment distribution simulated by the primitive model

the runoff volume at the outlet as shown in Fig. 9

To overcome these problems we consider the transportation capacity based on the USP. The temporal change of distribution is shown in Fig. 10 and the total volume of sediment yield is shown in Fig. 9 by the USP model. Because a total volume of sediment yield after a rainy season is much smaller than the result by the primitive model, it is quite difficult to visualize the sediment depth change. We confirmed that the steep slopes yields more sediment than gentle slopes. The total volume of sediment yield 40,000 m^3 is more adequate than that obtained by the primitive model. Another 80,000 m^3 contributing to the sediment

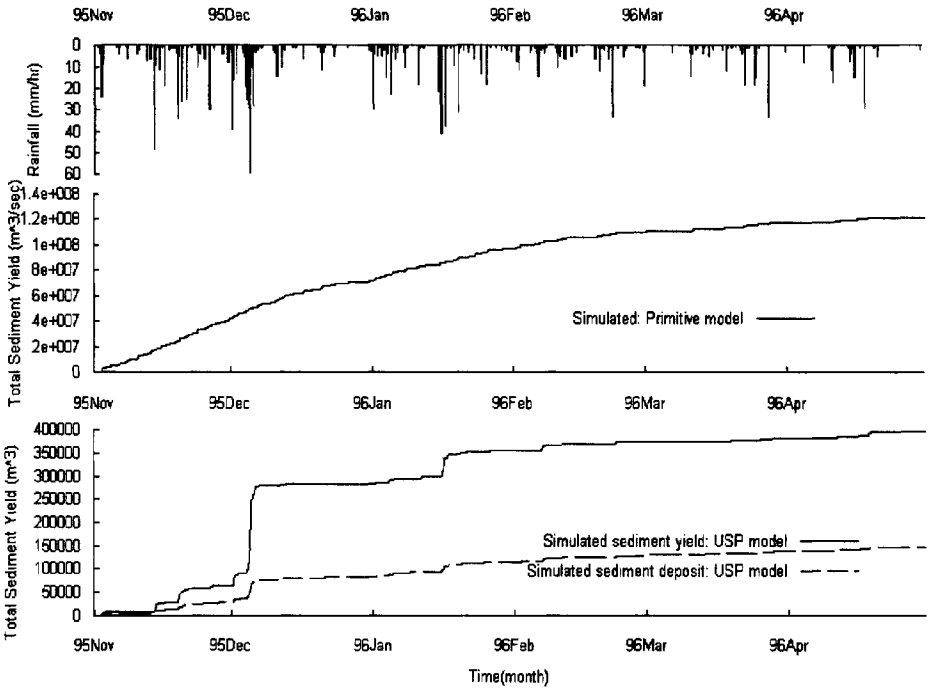

Fig. 9 Sediment yield of the whole basin

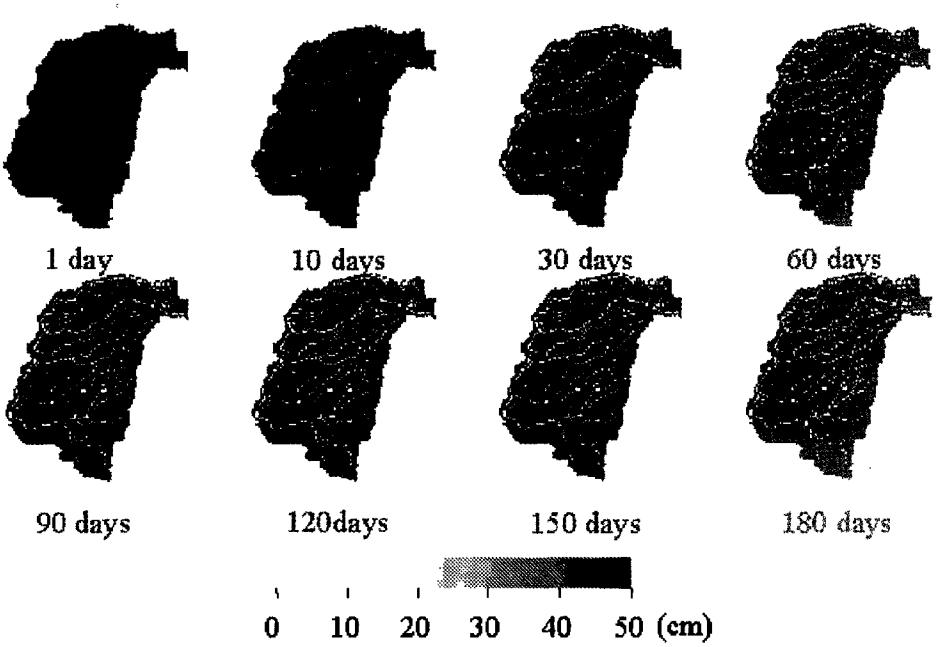

Fig. 10 Sediment distribution simulated by the USP model

runoff has been yielded on slope cells; Fig. 9 explains that the volume of deposited sediment is about 15,000 m^3 after a rainy season.

8. Conclusions

This paper has introduced a distributed rainfall-sediment-runoff model based on the kinematic wave runoff theory combined with the unit stream power theory to calculate transportation capacity of overland flow. GIS and RS were effec-

tively used to treat geographical data and land-cover classification for constructing this model. The model could reproduce the sediment runoff in the Lesti River basin.

Though more considerations about modeling and parameter settings are necessary to obtain more accurate sedimentation estimation, this kind of approach can give useful information for prevention and mitigation of flood and sediment disasters not only in Indonesia but other areas that are suffering from similar problems.

Acknowledgment

This research is a follow-up of Japan-Indonesia IDNDR (International Decade for Natural Disaster Reduction) Project conducted in 1991-1998. The authors are grateful for the support by the Grant-in-Aid for Scientific Research (B)(2) No.12574018 (Principal Investigator: Prof. Takara, Kyoto Univ.).

References

Abbott, M. and Refsgaard, C. (1996): *Water Science and Technology Library, Distributed Hydrological Modeling*, Kluwer Academic Publishers, Inc., pp. 93-120.

Ashida, K. and Michiue, M. (1972): Study on hydraulic resistance and bed-load transport rate in alluvial streams, *Proc. JSCE*, No. 206, pp. 59-69 (in Japanese).

Egashira, S. et al. (1997): Research on disasters due to floods and geomorphological change and their mitigation, *Annuals, DPRI, Kyoto University*, No. 40 IDNDR S.I., pp. 35-45 (in Japanese with English synopsis and captions).

Hirano, M. (1990): Runoff analysis considering surface runoff occurrence area, *Studies on Sediment Yield*, Sediment Yield Research Group, Committee on Hydraulics, JSCE, pp. 1-4 (in Japanese).

Hirano, M., Hikita, M. and Moriyama, T. (1986): Occurence criterion and discharge prediction of debris flow in the active volcanic area, *Proceedings of the 30th Japanese Conference on Hydraulics*, pp. 181-186 (in Japanese).

Jitousono, T. Shimokawa, E. (1989): Surface runoff on tephra-covered hillslope in Sakurajima volcano, *Journal of the Japan Society of Erosion Control Engineering*, Vol. 42, No. 3, pp. 18-23 (in Japanese).

Jitousono, T. et al. (1996): Distribution of ash fall deposit and infiltration rate on the flank of Unzen volcano, *Journal of the Japan Society of Erosion Control Engineering*, Vol. 49, No. 3, pp. 33-36 (in Japanese).

Kojima, T. (1997): *Application of remote sensing and GIS to hydrological analysis*, Dr. of Engineering Dissertation, Kyoto University (in Japanese).

Lane, E. W. and Kalinske, A. A. (1941): Engineering calculation of suspended sediment, *Trans. A. G. U.*, 22, pp. 603-607.

Moore, I. D., and G. J. Burch (1986): Sediment transport capacity of sheet and rill flow, *Water Resources Research*, Vol. 22, No. 8, pp. 1350-1360.

NASDA (1997): *Adeos Reference Handbook.*

Onda, Y. et al. (1996): The mechanism inducing the infiltration rate lowering of Unzen volcanic ash, *Journal of the Japan Society of Erosion Control Engineering*, Vol. 49, No. 1, pp. 25-30 (in Japanese).

PERUM JASA TIRTA (1994): Joint research proposal on sediment runoff in the Brantas basin, *Research Institute for Water Resource Development, Ministry of Public Works, and Kyoto University.*

Roedjito, D.M. and Harianto (1995): Controlling reservoir sedimentation in Sengguruh Reservoir, Brantas River Basin, *Reservoirs in River Basin Development, Proceedings of the Icold Symposium Oslo Norway.*

Shiiba, M. (1983): *Fundamental studies on modeling and prediction of runoff systems*, Dr. of Engineering Dissertation, Kyoto University (in Japanese).

Takara, K. et al. (1996): Application of remote sensing and GIS to research on disasters caused by floods and sedimentation, *Proc. Workshop on Disasters Caused by Floods and Geomorphological Changes and Their Mitigations (WDFGM-1996)*, pp. 62-77.

Takara, K. (2000): Remote sensing and GIS application to modeling of flood and sediment runoff in the Brantas River basin, Indonesia, *Proc. Second Workshop on Remote Sensing of Hydrological Processes & Apprications*, pp. 21-34.

Yang, C.T. (1996): *Sediment Transport Theory and Practice*, The McGraw-Hill Companies, Inc.

要　旨

流域規模での洪水、土砂動態の把握を目的として分布型洪水・土砂流出モデルを構築する。分布型モデルは空間分布情報を取り扱うため、GIS やリモートセンシングの応用が有効である。本研究では DEM の作成とその他の地理情報の取り扱いに GIS を、土地被覆分類にリモートセンシングを用いる。構築される流出モデルはセル分布型の土砂流出モデルであり、火山灰堆積地において表面流が発生したときに土砂が生産される。従来のモデルでは雨水浸透厚の厚さで土砂が生産されると仮定していたが、本研究では表面流のもつ unit stream power に着目し輸送可能土砂量を計算した。これにより、土砂生産過程だけではなく土砂堆積過程をも考慮できるモデルへと改良することができた。構築されたモデルをインドネシア、ブランタス川上流部のレスティ川流域に適用し、1995 年 11 月から 1996 年 4 月の一雨季の降雨を入力することにより土砂流出計算を行い、モデルの性能についての検討を加えた。

キーワード：ブランタス川，洪水土砂流出モデル，*unit stream power*，*GIS*，*ADEOS/AVNIR*